Journal of Physics: Conference Series **190** (2009) 012054 doi:10.1088/1742-6596/190/1/012054

Retrieving photochemically active structures by time-resolved EXAFS spectroscopy

Renske M. van der Veen[1,2], Christian Bressler[1,2,3], Chris J. Milne[1], Van-Thai Pham[1], Amal El Nahhas[1], Frederico A. Lima[1], Wojciech Gawelda[1,4], Camelia N. Borca[2], Rafael Abela[2] and Majed Chergui[1]

[1] Laboratory of Ultrafast Spectroscopy, Ecole Polytechnique Fédérale de Lausanne, Switzerland
[2] Swiss Light Source, Paul Scherrer Institut, Switzerland
[3] *Now at:* European XFEL Project Team, Deutsches Elektronen Synchrotron, Germany
[4] *Now at:* Laser Processing Group, Instituto de óptica, CSIC, Spain

E-mail: majed.chergui@epfl.ch, renske.vanderveen@psi.ch

Abstract. Describing the nature and structure of molecular excited states is important in order to understand their chemical reactivity and role as intermediates in photochemical reactions. The recent implementation of x-ray absorption spectroscopy in the ultrafast time domain allows studying the electronic and structural dynamics of photochemically active molecules in solutions. In this work we present the structural determination of a photoexcited diplatinum molecule, $[Pt_2(P_2O_5H_2)_4]^{4-}$, which plays a photocatalytic role in important chemical conversions. A novel analysis of time-resolved EXAFS spectra based on the fitting of the experimental transients obtained from optical pump/x-ray probe experiments has been performed to derive a contraction of 0.31(5) Å of the two Pt atoms and a ligand expansion of 0.010(6) Å. The former is assigned to the formation of a transient Pt-Pt bond in the excited state, while the latter indicates a concomitant weakening of the Pt-ligand coordination bonds.

1. Introduction

Over the last few years time-resolved x-ray absorption spectroscopy (XAS), exploiting short laser and x-ray pulses in a pump/probe scheme, has evolved to an established technique to retrieve electronic and geometric information about short-lived excited states of molecules in solution, in particular of transition-metal complexes with various organic ligands [1, 2, 3, 4]. These complexes are finding many applications, in the conversion of light energy into chemical energy, the storage and processing of optical and/or magnetic information, or as homogeneous photocatalysts in chemical conversions at room temperature [5]. The function of the excited systems is often strongly correlated with their transient structure, which makes the elucidation of the latter of paramount importance for the understanding of their chemical reactivity and role as active species in photochemical conversions.

The time resolution necessary to study excited states is based on the pump/probe scheme, in which a 100 fs laser pulse excites the sample and the x-ray transmission or fluorescence is recorded with $\sim$ 70 ps pulses at twice the repetition rate of the laser (typically 1 kHz) [6]. In this way, the difference between excited state and ground state XAS spectra is measured on a rapid shot-by-shot basis, enhancing the sensitivity by eliminating long-term drifts.

While rapid experimental improvements broaden the range of chemical systems and processes that can be studied by time-resolved XAS, developments on the theory side are necessary to retrieve precise structural information from time-resolved XAS spectra. Here we present a novel data analysis procedure based on fitting the transient (excited - unexcited) EXAFS spectrum directly in energy space, which has been shown to give superior accuracy of the derived structural parameters compared to conventional methods that rely on fitting the Fourier Transform of the excited-state EXAFS signal [7]. This method has been applied to the transient L_3-edge EXAFS spectrum of the photoexcited $[Pt_2(P_2O_5H_2)_4]^{4-}$anion with the aim of retrieving the structural distortions that occur upon excitation in its photocatalytically active excited state [8].

2. Experimental setup

The laser pump / x-ray probe measurements were performed at the microXAS beam line of the Swiss Light Source at the Paul Scherrer Institute. A 10 mM solution of $TBA_4[Pt_2(P_2O_5H_2)_4]$ (TBA = tetrabutylammonium) in degassed ethanol was flown in a thin quartz capillary of 500 μm path length. The sample was excited with 100 fs laser pulses at 390 nm from a tunable laser OPA (50 mW, 1 kHz), while $\sim$ 70 ps monochromatic tunable hard X-ray pulses probe the system as a function of adjustable pump-probe time delay. The experimental setup is described in detail elsewhere [6, 9].

3. A novel data analysis approach for transient EXAFS spectra

The quantitative structural analysis of the excited state that we performed is based on fitting the recorded difference (excited - unexcited) XAS spectrum directly in energy space [7], in contrast to conventional methods that rely on fitting the (weighted) Fourier Transform of the k-space EXAFS data. Our approach reduces the number of required parameters by cancellation in the differences. In addition, it allows to introduce the excitation yield (fractional excited state population) as a fitting parameter, which is especially useful in cases where the excitation yield can not be accurately derived by optical pump-probe measurements. The second point in which this analysis differs from usual fitting procedures lies in that we calculate the EXAFS signal for each excited state structure separately. In a usual EXAFS analysis, the *ab initio* FEFF [10] calculation is performed once for a structure that is thought to be close to the structure of the system under study, after which the structure parameterization and fitting are carried out. This approach requires a substantial amount of prior knowledge about the structure because only small deviations from the input structure are allowed, and the structural parameterization should respect the chemical integrity of the system, often resulting in complicated expressions for the structural parameters. Here, we allow the excited state structure to change by large amounts in a chemically sensible way, in that we perform a FEFF calculation for every structure separately while no complicated structural parameterization is required.

3.1. Data treatment and statistical analysis

Prior to the theoretical analysis, the raw x-ray fluorescence-excitation difference spectra at different time delays after excitation were normalized to the incoming intensity and subsequently divided by the fluorescence edge jump magnitude. The resulting normalized signal $\Delta A(t, E)$ represents the *transient* EXAFS function $\Delta\chi(E)$ scaled by the time-dependent excitation yield $f(t)$, according to

$$\Delta A(t, E) = f(t) \cdot [\chi_{ES}(E) - \chi_{GS}(E)] = f(t) \cdot \Delta\chi(E) \ , \tag{1}$$

where $\chi_{ES}(E)$ and $\chi_{GS}(E)$ are the EXAFS functions of the excited state and ground state structures, respectively. In the following we consider the difference XAS spectrum at a certain time-delay after time zero, which is justified for the case of a single intermediate excited state

with a life time that is long compared to the ∼70 ps x-ray pulse. The procedure can be generalized for the case of evolving transient structures and superimposed intermediate states in a multi-step relaxation pathway [7]. EXAFS signals $\chi^i_{ES}(\Delta R_i, k)$ for a series of i possible excited state structures are generated by using the FEFF6 code [10] included in the IFEFFIT software package [11] (the structural distortion compared to the ground state is denoted by ΔR_i). The $\chi^i_{ES}(\Delta R_i, k)$ signals are generated by using the same structural parameterization model as for the ground state, i.e. the same scattering paths, amplitude reduction factor S_0^2, energy shift E_0 and the Debye-Waller factors σ^2 are used. After conversion into energy space, the ground state EXAFS fit $\chi^{fit}_{GS}(E)$ is subtracted resulting in the theoretical differences

$$\Delta\chi^i(\Delta R_i, E') = \chi^i_{ES}(\Delta R_i, E') - \chi^{fit}_{GS}(E) \ , \tag{2}$$

with $E' = E + \Delta E_0$, which are compared to the experimental difference signal $\Delta A(E)$ in a non-linear least-squares fitting procedure for a series of excitation yields f and energy shifts ΔE_0 between excited state and ground state XAS spectra. The latter, so-called chemical shift, can be caused by a change in the ionization threshold as a result of the light-induced structural changes. The statistical figure that provides the quality of the fit is the normalized square residual

$$R^2(\Delta R_i, f, \Delta E_0) = \frac{1}{N-1}\sum_{j=1}^{N}\left(\frac{x_j/f - \Delta\chi^{i,j}(\Delta R_i, E')}{\sigma^x_j/f}\right)^2 \tag{3}$$

within the limited range of experimental data points j (total N data points), where σ^x_j represents the standard deviation of experimental data point x_j.

4. Retrieving photochemically active structures

The above fitting procedure has been applied to determine the structural changes that occur upon excitation of the bridged μ-pyrophosphato diplatinum(II) complex $[Pt_2(P_2O_5H_2)_4]^{4-}$, which exhibits the richest excited-state chemistry of all binuclear d^8-d^8 complexes [12, 13]. The photo-physical and -chemical properties of these complexes are a manifestation of the newly formed bond in the lowest excited singlet and triplet $^{1,3}A_{2u}$ states, owing to the promotion of an electron from the antibonding dσ^* ($5d_{z^2}$-derived) to the bonding pσ ($6p_z$-derived) orbitals. The key question towards understanding the photoreactivity of these complexes is therefore the structure of the triplet excited state.

Figure 1 shows the static L_3 edge absorption spectrum of $[Pt_2(P_2O_5H_2)_4]^{4-}$in the ground state as well as the transient XAS spectrum integrated up to 150 ns after excitation. A simultaneous measurement of the time dependence of the transient XAS signal and the optical phosphorescence around 550 nm showed the same ∼1 μs decay, which confirms that the changes in the XAS spectrum up to 150 ns after excitation are inevitably due to the electronic and molecular structure changes in the triplet $^3A_{2u}$ state. This is further supported by the appearance of a new absorption feature in the XANES spectrum around 11.574 keV, caused by the creation of a hole in the 5dσ^* orbital upon laser excitation, which can then be accessed from the $2p_{3/2}$ core orbital (L_3 edge). In the following we focus on the changes in the EXAFS region of the spectrum, from which we can directly extract the magnitude of the Pt-Pt bond contraction as well as, for the first time, the changes affecting the ligand coordination bonds.

4.1. Structural parameterization

The first step in the analysis is the refinement of the ground state structure and non-structural EXAFS parameters such as the amplitude reduction factor S_0^2, energy shift E_0 and the Debye-Waller factors σ^2. In the case of $[Pt_2(P_2O_5H_2)_4]^{4-}$, the following structural parameterization model is used [14]: single scattering paths up to the third shell are included, consisting of single

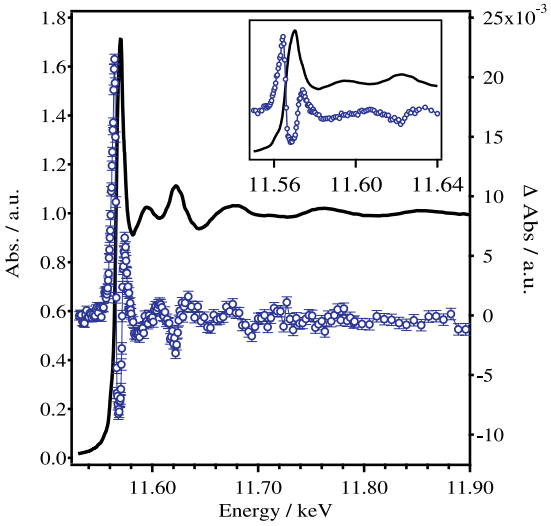

Figure 1. Static Pt L_3 XAS spectrum of in solution (black line, left axis) and the transient (excited-unexcited) XAS spectrum (blue circles, right axis, same units as left) integrated up to 150 ns after excitation. The inset zooms into the XANES region.

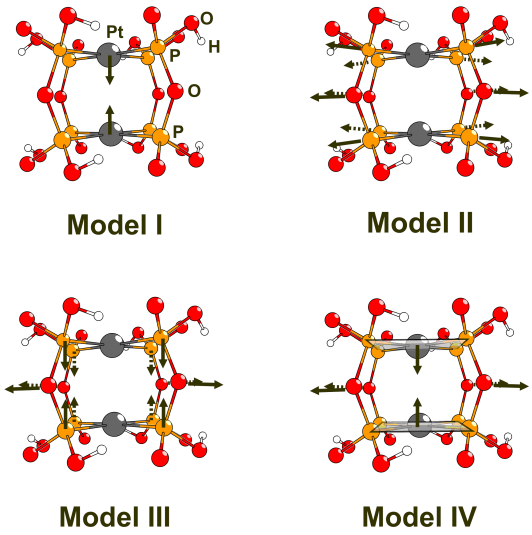

Figure 2. Schematic representation of the structural distortion models I-IV considered in the statistical analysis (distortion indicated by arrows). The bridging P-O bond lengths are fixed for the distortions of models III and IV.

scattering from Pt to the near P atoms (1st shell), the bridging and terminal O-atoms (2nd and 4th shell), the far P atoms (3rd shell) and the second Pt atom. One important collinear multiple scattering path via Pt-P-Pt-P is included as well. It should be pointed out that the different scattering paths in the second shell (bridging O atoms and the second Pt atom) and third shell (P atoms in the opposite plane) have a comparable magnitude. The Debye-Waller factors of the ground state fit are used to simulate the EXAFS signals of the excited state, because they are not expected to change considerably between ground and excited states. They are: σ^2(P near) = 0.0031 Å^2, σ^2(O bridging) = 0.0007 Å^2, σ^2(P far) = 0.0105 Å^2, σ^2(Pt) = 0.0053 Å^2 (fixed [14]), σ^2(O terminal) = 0.03 Å^2. In addition, an amplitude reduction factor of S_0^2=0.94 and an E_0 shift of 7.4 eV were used.

4.2. Model-based fitting of the transient EXAFS spectrum

The fitting procedure as described in section 3 relies on additional knowledge about the possible structural changes that can occur upon excitation. The distortions need to be chemically reasonable respecting the nature of the optical excitation, while ample variation in their magnitude is allowed. Ideally, this approach reduces the degrees of freedom considerably, and therefore it allows finding an unambiguous solution for the excited-state structure and extracting additional information, such as the chemical shift and excitation yield.

The antibonding-to-bonding 5dσ^*→6pσ nature of the electronic transition led us to consider only structural distortions that involve a contraction along the Pt-Pt axis. As to whether and how the ligands are influenced by the excitation, four chemically reasonable deformation models are applied (Figure 2).

- **Model I**: In-/outwards movement of the Pt atoms along the Pt-Pt axis, while the ligands stay in place. The P-O-P angles do not change. This necessarily implies a small increase in the Pt-P bond lengths and a change in P-Pt-P bond angle.
- **Model II**: Contraction/expansion movement of the P-O-P bridging ligands along the Pt-P coordination bonds. The P-O-P angles do not change (thus the distance between both ligand planes is fixed).
- **Model III**: Contraction of the P_4 planes along the Pt-Pt axis while the P-O bonds within the ligands are kept fixed (strong covalent bonds not expected to change). This necessarily implies an outward movement of the bridging O atoms and a consequent change in P-O-P angle.
- **Model IV**: The Pt atoms stay in the plane of the P atoms as the molecule contracts along the Pt-Pt axis. Again, the P-O bonds are kept fixed and the P-O-P angle decreases, while the Pt-P bond lengths do not change. This model was suggested as a mode of distortion in references [15, 16].

The first two distortion models are tested in an iterative way: (1) Model I is applied to the ground state structure in steps of 0.01 Å which results in an absolute minimum of $R^2 = 1.67$ at 0.31 Å Pt-Pt contraction, 8% excitation yield and a -1 eV energy shift; (2) the P-O-P contraction/expansion movement according to Model II is then applied in steps of 0.002 Å while the Pt-Pt contraction is kept at 0.31 Å, from which a new minimum of $R^2 = 1.39$ at 0.010 Å distortion, 7% excitation yield and zero energy shift was obtained; (3) an optimization of the Pt-Pt contraction was again performed, but now with the P-O-P expansion fixed to 0.010 Å. This last step yields an $R^2 = 1.39$ minimum for a Pt-Pt contraction of 0.31 Å, a 7% excitation yield and zero energy shift, confirming the results of step (2), so that no new iteration of the P-O-P contraction/expansion movement was necessary. The R^2 dependencies according to Equation 3 for the combined distortions of Models I and II are shown in Figure 3 (after convergence of the fit). The errors of the structural distortions belonging to the minima are obtained by taking a

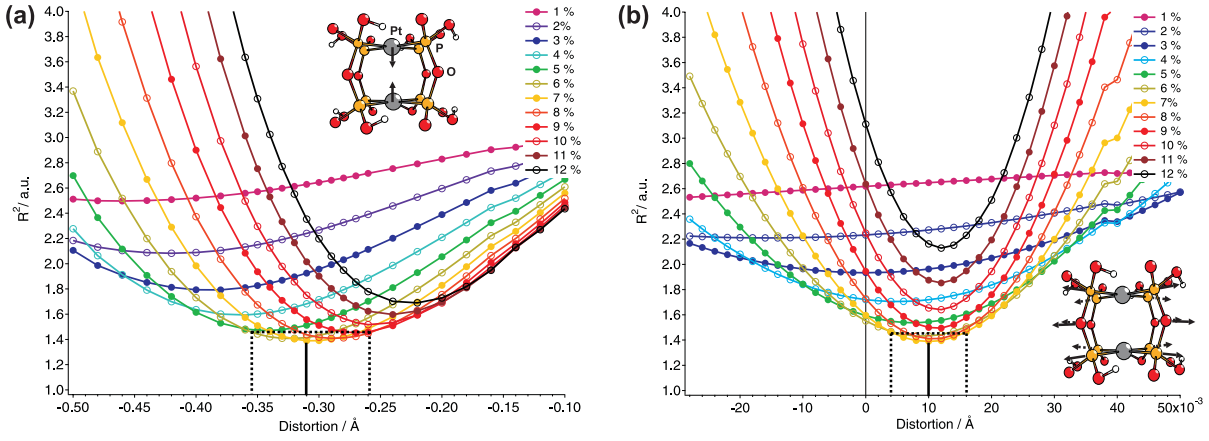

Figure 3. R^2 dependencies according to Equation 3 as a function of distortion and excitation yield after iterative optimization of the fit by changing the structure according to Models I and II; (a) R^2 dependence as a function of Model I (negative = reduced Pt-Pt distance) for a series of excitation yields and a fixed POP expansion of 0.010(6) Å ($\Delta E_0 = 0$); (b) R^2 dependence as a function of Model II (positive = increased Pt-P distance) for a series of excitation yields and a fixed Pt contraction of 0.31(5) Å ($\Delta E_0 = 0$). The solid vertical lines denote the absolute minima in the 4-parameter space (ΔPt-Pt, ΔPt-P, ΔE_0, f), while the dashed lines show the significance level of 5%.

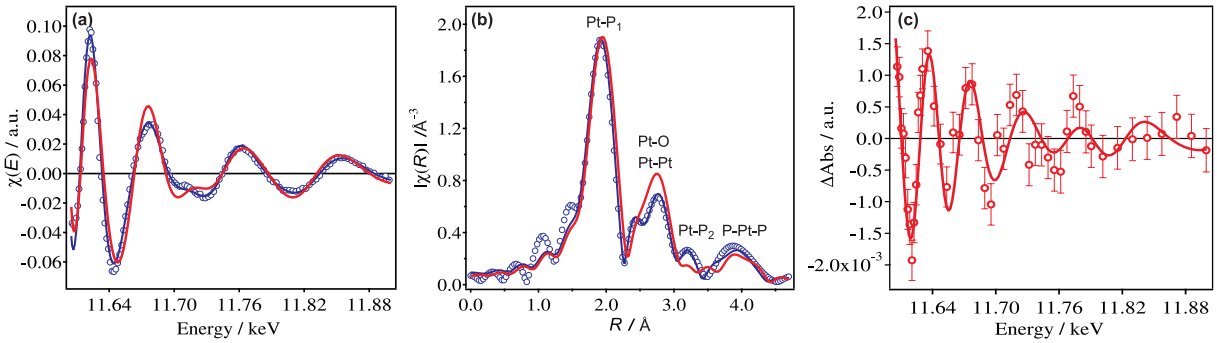

Figure 4. (a) Ground state EXAFS data $\chi_{GS}(E)$ with best fit (blue circles and line) and best-fit excited state EXAFS signal $\chi_{GS}(E)$; (b) Fourier transform of the data in (a) with the assignment of scattering pathways (same color assignment, P_1 is the P shell closest to the absorbing Pt atom, P_2 are the third-shell atoms); (c) Transient EXAFS data integrated up to 150 ns after excitation (red circles) and the best fit after iterative optimization according to distortion models I and II (see text)

R^2 significance level of 5%, as is indicated by the dotted lines in Figure 3. R^2 values were also calculated for energy shifts between -5 to 5 eV, but they resulted in significantly higher values over the whole distortion range. The result of the best fit is shown in Figure 4 together with the ground state data and Fourier transform spectra.

The 7% excitation yield obtained from the fit is in good agreement with the one estimated (∼8%) from independent optical pump-probe measurements [8]. Furthermore, the fitted zero energy shift may be expected for a metal-centered transition without change of oxidation state of the absorbing metal.

A similar iterative optimization procedure was applied for the distortions according to Models III and IV (see Figure 5), which both test whether the P-O-P bridging ligands follow the Pt atoms in the contraction [15, 16]. The R^2-dependence of Model III shows only a very shallow minimum

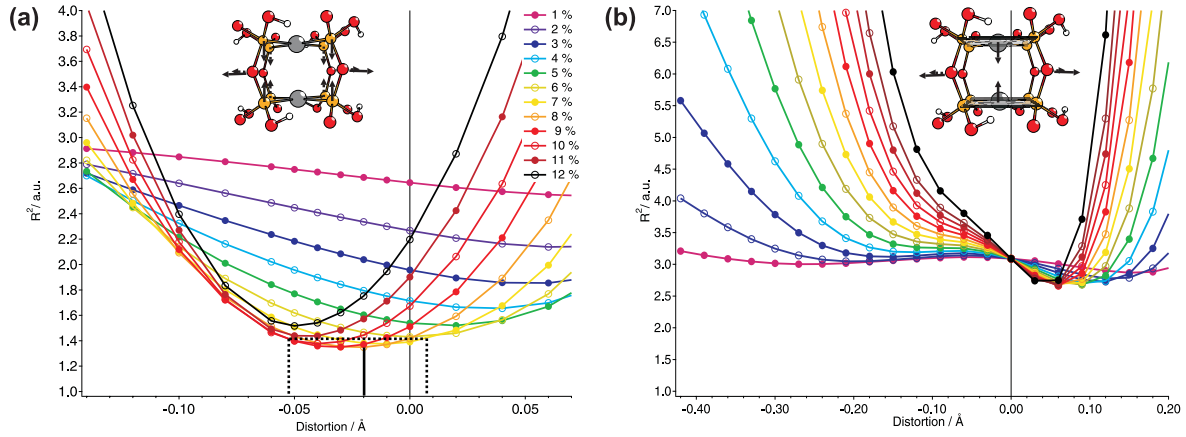

Figure 5. R^2 dependencies according to Equation 3 as a function of distortion and excitation yield after iterative optimization of the fit by changing the structure according to (a) Model III and (b) Model IV; (negative = reduced P_4 plane distance). The best-fit distortions of Models I and II were fixed.

around -0.02 Å, which is statistically not significant (within the 5% significance interval) and much smaller than the contraction of the Pt atoms (0.31 Å). Model IV can be rejected based on the generally much higher R^2 values compared to Models I-III.

5. Conclusions

The present study demonstrates that accurate structural changes in photoexcited molecules can be determined by fitting the transient EXAFS spectrum directly in energy space and that additional non-structural information, such as the excitation yield and chemical shift, can be extracted from the fit due to the largely reduced parameters space in a model-based analysis as is shown here. There are no limitations on the magnitude of the distortions and no complicated parameterization of the scattering paths is necessary, because the EXAFS signal of every (chemically reasonable) excited-state structure is calculated separately.

The analysis has been applied to the transient L_3-edge EXAFS data of the photoexcited $[Pt_2(P_2O_5H_2)_4]^{4-}$anion. A rigorous statistical comparison of several different excited state structures according to distortion models that involve a contraction along the Pt-Pt axis resulted in a best-fit distortion involving mainly the heavy Pt atoms (contraction by 0.31(5) Å) and a small Pt-ligand elongation of 0.010(6) Å. Remarkably, the bridging P-O-P ligands do not follow the heavy Pt atoms in their contraction, which indicates weak(ened) Pt-ligand coordination bonds and rigid bridging ligands.

Time-resolved EXAFS spectroscopy in combination with the herein proposed analysis approach is a promising method that can be extended into the fs regime to study the chemical transformations of non-equilibrium transition states.

Acknowledgements

We thank T. Vlček and S. L. Johnson for useful discussions, D. Grolimund and H. Brands for assistance during the experiment and J.A. Weinstein, J. Best and E. Baranoff for synthesizing the sample. This work has been supported by the Swiss SBF in the COST D35 action via grant 06.0016 and was funded by the Swiss National Science Foundation via Contract Nos. 620-066145, 200020-116023, 200021-16894 and 200021-105239.

References

[1] Chergui M and Zewail A H 2009 *Chemphyschem* **10** 28–43
[2] Bressler C and Chergui M 2004 *Chem. Rev.* **104** 1781–1812
[3] Chen L X 2004 *Angew. Chem. Int. Ed.* **43** 2886–2905
[4] Bressler C, Abela R and Chergui M 2008 *Zeitschrift fur Kristallographie* **223** 307–321
[5] Vlcek A 2000 *Coord. Chem. Rev.* **200** 933–977
[6] Gawelda W, Pham V, Nahhas A E, Kaiser M, Zaushitsyn Y, Johnson S, Grolimund D, Abela R, Hauser A and Bressler C 2007 *J. Phys.: Conf. Series* **882** 31–36
[7] Gawelda W, Pham V T, van der Veen R M, Grolimund D, Abela R, Chergui M and Bressler C 2009 *J. Chem. Phys.* **130** 124520
[8] van der Veen R M, Milne C J, Nahhas A E, Lima F A, Pham V T, Best J, Weinstein J A, Borca C N, Abela R, Bressler C and Chergui M 2009 *Angew. Chem. Int. Edit.* **48** 2711–2714
[9] Saes M, Bressler C, Mourik F V, Gawelda W, Kaiser M, Chergui M, Bressler C, Grolimund D, Abela R, Glover T, Heimann P, Schoenlein R, Johnson S, Lindenberg A and Falcone R 2004 *Rev. Sci. Instrum.* **75** 24–30
[10] Rehr J and Albers R 2000 *Rev. Mod. Phys.* **72** 621–654
[11] Ravel B and Newville M 2005 *J. Synchrotron. Rad.* **12** 537–541
[12] Zipp A 1988 *Coord. Chem. Rev.* **84** 47–83
[13] Roundhill D, Gray H and Che C 1989 *Acc. Chem. Res* **22** 55–61
[14] van der Veen R M, Milne C J, Pham V T, Nahhas A E, Weinstein J A, Best J, Borca C N, Bressler C and Chergui M 2008 *CHIMIA* **62** 287–290
[15] Fordyce W, Brummer J and Crosby G 1981 *J. Am. Chem. Soc.* **103** 7061–7064
[16] Thiel D, Liviņs P, Stern E and Lewis A 1993 *Nature* **362** 40